Fisheries Research 109 (2011) 114–118

Contents lists available at ScienceDirect

Fisheries Research

journal homepage: www.elsevier.com/locate/fishres

Differences in acoustic target strength pattern between fish with one- and two-chambered swimbladder during rotation in the horizontal plane

Jaroslava Frouzova*, Jan Kubecka, Tomas Mrkvicka

Biological Center AS CR, v.v.i., Hydrobiological Institute, Na Sadkách 7, Ceské Budejovice, Czech Republic

ARTICLE INFO

Article history:
Received 30 September 2010
Received in revised form 24 January 2011
Accepted 24 January 2011

Keywords:
Target strength
Fish
Swimbladder
Horizontal
Acoustics

ABSTRACT

Pattern of target strength (TS) during 360° rotation in the horizontal plane was studied for six common European fish species: brown trout (*Salmo trutta*), perch (*Perca fluviatilis*) bream (*Abramis brama*), roach (*Rutilus rutilus*), carp (*Cyprinus carpio*), and bleak (*Alburnus alburnus*). Trout and perch have one-chambered swimbladders, and the other species have two-chambered swimbladders. In general, the lowest TS was recorded when the head or tail faced the sonar beam and the highest values when the side was perpendicular to the sonar beam. The TS distribution differed between fish with one- and two-chambered swimbladders. For two-chambered fish, the TS transition between minima and maxima was linear, and the median of the TS value was similar to the mean. For one-chambered fish, TS distribution was skewed and the median TS was considerably smaller than the mean. The relationship between TS and fish aspect relative to the sonar beam, can be described by a linear model for fish with two-chambered swimbladders and by a quadratic model for fish with one-chambered swimbladders. This study provides new general equations for modeling the dependence of TS on any body aspect in the horizontal plane as well as equations for common European fish species.

1. Introduction

Acoustical observation of the fish stocks in both freshwater (Kubecka and Wittingerova, 1998; Knudsen and Seagrov, 2002) and saltwater (Pedersen et al., 2009) often depends on a horizontally directed sonar. When observed horizontally, the orientation of the body axis of the fish in relation to sound beam axis is not known, i.e., the fish may be observed at any position along a 360° circle (Tuser et al., 2009). The aspect of the fish relative to the sound beam greatly influences the target strength (TS) (Frouzova et al., 2005). Target strength is highest when the side of the fish is perpendicular to the sonar beam (side aspect), and lowest when the fish is in head or tail aspect.

The difference between maximum and minimum TS as a consequence of fish aspect is usually more than 20 dB (Kubecka, 1994; Frouzova et al., 2005) and it can lead to under- or overestimation of fish size and consequently to under- or overestimation of the biomass of the fish population.

Kubecka (1994) and Lilja et al. (2000) reported that when a fish turns on a horizontal plane relative to the sonar sound beam, a plot of TS values produces a sinusoidal curve. Lilja et al. (2000) adjusted this equation by including the effects of body length and another constant, which varied with fish species (salmon, pike and whitefish). In a “carousel experiment”, in which fish are turned on a horizontal plane relative to a sonar beam, Frouzova et al. (2005) suggested that the TS pattern might differ between fish species with one- and two-chambered swimbladders. The current study is a continuation of the carousel experiment (Frouzova et al., 2005). The first aim of this study was to determine whether the TS pattern generated when fish turn 360° relative to a sonar beam differed between fish with one- and two-chambered swimbladders and whether these differences vary with fish size. The second aim was to develop general equations for modeling the dependence of TS on any body aspect in the horizontal plane as well as to develop equations for common European fish.

2. Materials and methods

2.1. Materials

All data were collected in a concrete pond of 12 × 5 × 2 m (length × width × depth) using a “fish rotating carousel” (Frouzova et al., 2005). The fish used in the experiment belonged to the families Salmonidae – brown trout (*Salmo trutta*); Percidae – perch (*Perca fluviatilis*); and Cyprinidae – bream (*Abramis brama*), roach (*Rutilus rutilus*), carp (*Cyprinus carpio*), and bleak (*Alburnus alburnus*). All of these fish have a plain, cylindrical swim bladder but trout and perch have one-chambered swim bladders whereas the other

* Corresponding author. Tel.: +420 387775870; fax: +420 385310248.
E-mail address: jfrouzova@yahoo.com (J. Frouzova).

0165-7836/$ – see front matter © 2011 Elsevier B.V. All rights reserved.
doi:10.1016/j.fishres.2011.01.026

species have two-chambered swimbladders. The fish ranged from 72 to 710 mm in total length and from 4 to 6913 g in body mass. The species and size ranges are representative of the fish commonly found in fresh water reservoirs in Central Europe.

2.2. Experimental setup

The experimental setup was described in detail in Frouzova et al. (2005). All fish were stored for up to 2 days in an aerated 1000 l tank before the experiment. Each fish was anesthetized with MS 222 (Sandoz) immediately before the experiment, and its total length was measured. The fish was then mounted in the carousel. The frame, with the still anesthetized fish, was then mounted on the rotator with the side of the fish facing the sonar transducer (see next section); this aspect of the fish relative to the transducer was defined as 90°. The distance between the fish and the transducer was about 6 m. The transducer's pan and tilt were trimmed so that the fish were exactly aligned with the acoustic axis of the beam. With the carousel always rotating counterclockwise, all fish thus produced the same sequence of side, head, side, and tail. Several turns were recorded. The pinging of the echosounder and the rotation of the carousel were started simultaneously. One complete rotation took about 4 min. With a ping rate of 10 pings per second, 2400 measurements were obtained from each cycle.

2.3. Acoustic equipment and measurement

A Simrad EY 500 split beam echosounder recorded the acoustic data. The echosounder was equipped with an ES120-4 elliptical transducer (120 kHz sound frequency with a nominal beam angle of $9.1 \times 4.3^\circ$). The transducer was mounted on a remotely controlled Subatlantic pan and tilt rotator with the 'along ship' axis facing vertical in the water. The echosounder was set to store echo trace, sample angle, and sample power telegrams at a ping-rate of 10 pings per second. The duration of the transmitted pulse was 0.1 ms, and the bandwidth was set to 12 kHz (wide). The telegrams for storage of echograms were set to record 250 echo samples with a range of 15 m and with the TVG 40log R indicating a point-spread model. The attenuation coefficient was set to 6 dB km^{-1} (Francois and Garrison, 1982). The echosounder's single-echo-detector parameters were set to accept echoes with a minimum value of −72 dB (threshold), minimum echo length of 0.8, and maximum echo length of 1.5 times the transmitted pulse length. Maximum gain compensation was 5 dB, and maximum phase deviation was 10. Further explanation of these criteria is in the SIMRAD manual (1994). We used this wide setting to ensure capture of as many detections from fish as possible. The echosounder system was calibrated every day with a 23-mm copper calibration sphere located 6 m from the transducer in the same distance like the experimental targets, and background noise level peaked at around −75 dB.

2.4. Data processing

The raw echo data were first processed with Sonar5-Pro (Balk and Lindem, 2006) and then with MS Excel software as described in Frouzova et al. (2005). The echoes from two or more complete turns were processed. Single echo detections of fish were separated from noise detections. Only detections within ±3° on the 'athwart' axis and ±2° on the 'along ship' axis were accepted for processing.

Some statistical post-processing (descriptive statistics, correlations, regressions, and *t*-tests) was also carried out in Excel 6. The basic characteristics of a normal distribution, such as the skewness of the TS distribution of all records of fish rotating 360° in a horizontal plane (Fig. 1), were calculated using Statistica. The general linear model in Statistica was also used to compare the effect of fish species, fish size, and number of swimbladder chambers on skewness.

Table 1
Quadratic model M describes the TS pattern of fish. TS is target strength in dB. A (angle) indicates fish orientation or aspect toward the beam axis in degrees. The unknown parameters are a, b_1, b_2, c_1, and c_2. Linear model is submodel of the quadratic model with b_2 and $c_2 = 0$.

$M =$	$a + b_1 A + b_2 A^2$	$0 \le A \le 90$
	$a + b_1 90 + b_2 90^2 + c_1(A-90) + c_2(A-90)^2$	$90 \le A \le 180$

2.5. Modeling

All regression fits were non-linear and were produced by minimizing the sum of square with the least-squares method. The minimized functions were programmed in the software Mathematica. Searching for the most suitable model that described the TS pattern of fish in a horizontal beam began with the simplest case of one particular fish. A bream with a total body length of 203 mm was randomly chosen to be modeled first. The initial models for describing the TS pattern were the piecewise linear function or piecewise quadratic function, where the turning points are 0, 90, 180° (see Table 1). All models assumed that the data produced by fish aspects between 90 and 180° were identical to those produced between 270 and 360°. Similarly, all models assumed that data from 0 to 90° were identical to data from 180 to 270°.

The sine function was chosen for describing the peaks and valleys observed in the individual scattering response surface; such peaks and valleys are induced by constructive and destructive wave interference (Simmonds and MacLennan, 2005), which are sometimes called lobes (Love, 1977; Johannesson and Mitson, 1983) (Fig. 1). The amplitude and frequency of the sine function were varied to obtain the best fit between the observed and modeled data.

After the general model was developed, it was fitted for specific species or groups of fish. The general model was:

$$\mathrm{TS} = m \log L + M + n \log LM$$

where TS is the target strength at any aspect, L is total fish length, and M is the equation for linear or quadratic model for one of the fish defined above. Thus, the unknown parameters of the model are a, b_1, b_2, c_1, c_2, m, and n. The parameter m corresponds to the increase in TS with increase in fish length. The parameter n corresponds to the increase in the range of TS with increase in fish length (Frouzova et al., 2005).

The decision to use a linear or quadratic model for a particular species or group of fish was determined as follows. First, a quadratic model was constructed for one-quarter of the data (for example, with aspect angle 0–90°), and the usual methods for reducing the model were used (*t*-test).

This classical method did not reduce any parameter from any model (except one case), where it was used. This was caused by the enormous amount of the data, which resulted in every parameter, even those that had only minor effects in the model, being statistically significant. In such situations, one can add a weight for each new parameter, so that the weight added increases as more parameters are included in the model. Such weighting is usually used in the degree of polynomial estimation and is known as the Akaike criterion (Akaike, 1974). However, this criterion selected the simplest model in all our cases, even when the simplest model is clearly not the best choice. The lobes probably caused this.

Because of this statistical problem associated with the use of a linear model, a more complex model (a quadratic model) was selected if it increased the amount of explained variability by more than 0.5%. We assumed that a 0.5% increase was the smallest increase with practical significance. When both estimates of the

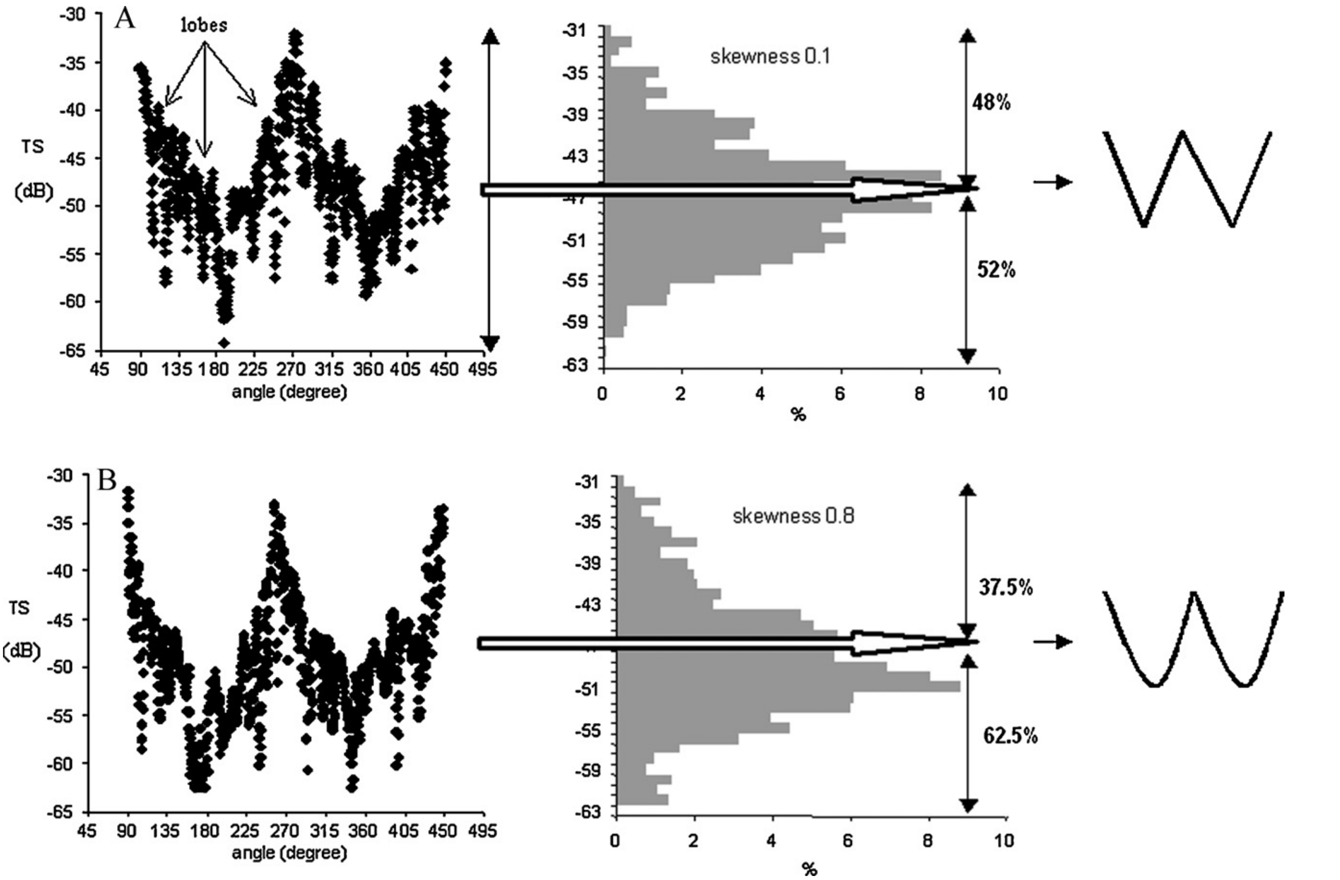

Fig. 1. Amplitude of TS pattern as fish is rotated 360° on a horizontal plane. Left graphs describe the TS pattern of a 190-mm-long carp (A) and a 200-mm-long trout (B). Right figures show the general patterns. Right graphs show the frequency distribution of the TS. In the middle graphs, horizontal arrows indicate half of the amplitude in TS variation, and values next to vertical arrows indicate the percentage of values that are greater than or less than the value for half of the amplitude.

response (linear and quadratic models) were drawn together, only those that fulfill above mentioned criteria were distinguishable in practical chart resolution.

3. Results

3.1. Distribution of TS values during one turn of the fish body along its vertical axis

When the fish was turned horizontally, TS values were strongest when the side of the fish was perpendicular to the sonar beam (90 and 270°) and weakest when the tail or head were oriented toward the beam (180 and 360°). The TS pattern produced by one turn of a carp (two-chambered swimbladder) and a trout (one-chambered swimbladder) is shown in Fig. 1.

TS patterns differed for fish with one- and two-chambered swimbladders (Figs. 1 and 2). The TS distribution of TS values above and below half of the TS amplitude clearly differed for these species in that the trout had more values in the lower half of the amplitude (Fig. 1B) while the carp had about the same number of values above and below the middle of the amplitude. We refer to these as the U-pattern distribution (Fig. 1B) and the V-pattern distribution (Fig. 1A).

The difference in TS pattern for fish with one- and two-chambered swimbladders is also evident in skewness, which was much higher for the trout than for the carp. If skewness of the TS distribution is plotted on TS for all investigated fish (rotated 360° in the horizontal plane), the plot indicates that skewness was not affected by TL but was significantly affected by the nature of the swimbladder, i.e., skewness was greater for fish

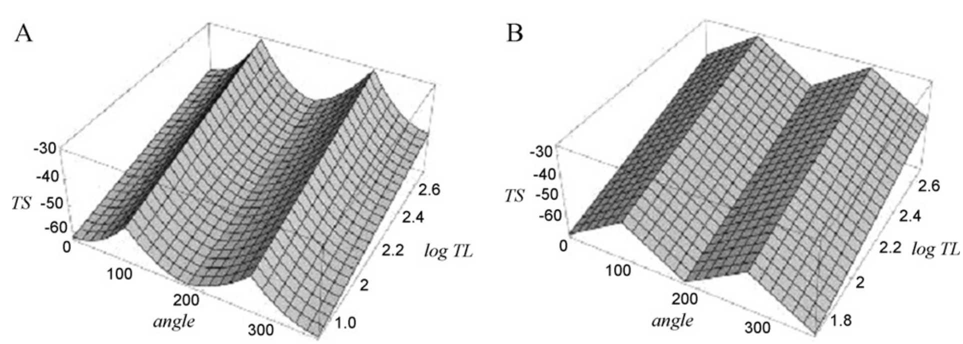

Fig. 2. Models of TS of fish with (A) one-chambered swimbladders and (B) two-chambered swimbladders.

Table 2
Coefficients of determination (R^2) for different species and different models. The preferred models are bolded.

Fish type	Number of fish studied	Linear model ($n=0$)	Quadratic model ($n=0$)	Linear model ($n \neq 0$)	Quadratic model ($n \neq 0$)
Bream	11	**0.6744**	0.6752	0.6745	0.6754
Carp	17	**0.7323**	0.7326	0.7324	0.7328
Bleak	5	0.5720	0.5771	0.5747	**0.5792**
Roach	8	0.6359	0.6435	0.6406	**0.6478**
Perch	6	0.5977	0.6056	0.5995	**0.6071**
Trout	9	0.5304	0.5642	0.5324	**0.5663**
Fish with two-chambered swimbladders	41	**0.6946**	0.6949	0.6946	0.6949
Fish with one-chambered swimbladders	15	0.5212	0.5407	0.5229	**0.5423**
All fish	56	0.6911	**0.6931**	0.6915	0.6934

with one- rather than two-chambered swimbladders (GLM test, Fig. 3). The same was true when the effect of TL and fish species on skewness was examined, i.e., skewness was not affected by TL ($p=0.829$) but was affected by fish species ($p=0.0007$, GLM test). One chambered swimbladder species (trout and perch) had higher skewness (0.54 ± 0.06 and 0.44 ± 0.07, respectively) than two-chambered swimbladder species, with roach > bleak > carp > bream ($0.32 \pm .15$, 0.27 ± 0.10, 0.13 ± 0.07, and -0.01 ± 0.10, respectively). In addition, no accentuation of lobes was observed for fish with two-chambered swimbladders (Fig. 1A) but was observed for fish with one-chambered swimbladders (Fig. 1B). The occurrence of lobes varied significantly among individual fish, and the number of lobes was not related to fish body length or number of chambers of the swimbladder (data not shown).

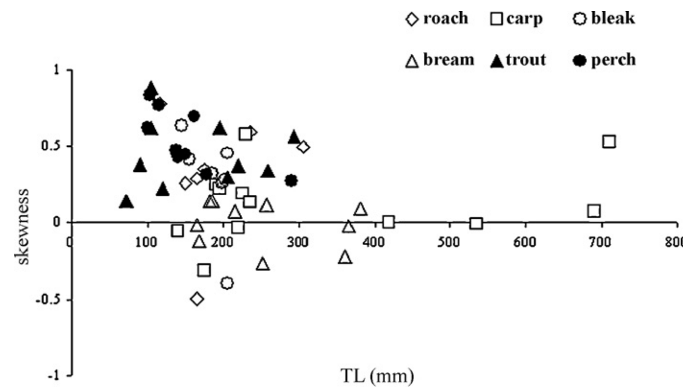

Source of variance	N	df	F	p
TL	55	1	0.27	0.6025
Number of swimblader chambers	55	1	14.72	0.0003

Fig. 3. Skewness of the TS (target strength) distribution of fish rotating 360° in the horizontal plane as a function of fish species and length (TL). The table shows results of a general linear models analysis that compared effect of TL and number of swimbladder chambers on skewness.

3.2. Modeling

The parameters of the general models (linear and quadratic) (Table 1) were estimated by the classical least-squares method. The linear and quadratic models were then created to describe the TS pattern for a particular species or groups of fish. The preferred models are shaded in Table 2, and the parameters for the preferred models were determined (Table 3).

Both of these models fit the trends of the TS patterns but did not describe the lobes. In an attempt to account for the lobes, a sine function was included, and the amplitude and frequency of the sine function was modified to obtain the best fit with the TS data. Any sine function, however, improved the fit for only some fish and always for only part of the data. It was not possible to improve the fit for all the data from one fish or from more than one fish. For these reasons, the lobes were not described by the model equations.

4. Discussion

The current study confirms that the shape of the fish swimbladder greatly affects TS (Horne and Clay, 1998). Our results indicate that the difference in TS pattern during rotation along the horizontal plane is associated with the number of swimbladder chambers, i.e., the TS pattern differs substantially between species with one- vs. two-chambered swimbladders. The reason for this difference is not known but perhaps the two-chambered swimbladder creates more opportunities for sudden overlapping of individual chamber echoes in near-side aspects during rotation, and such overlapping of echoes may result in higher TS values. Many studies have evaluated the effect of swimbladder shape and rotation on TS (McClatchie et al., 1996; Yasuma et al., 2003, 2006; Pena and Foote, 2008; Jaffe, 2006). Unfortunately, these studies were done in a vertical plane and for angles that are expected to occur in natural swimming only. Expanding these approaches to full rotation in horizontal plane will help elucidate observed differences between species with one- and two-chambered swimbladders.

We were unable to model the lobes in the TS response pattern. These lobes are produced by wave interference effects along

Table 3
Parameters of the preferred models for each species or group.

Fish type	Parameter						
	a	b_1	b_2	c_1	c_2	m	n
Bream	−87.6357	0.211695	0	−0.215638	0	14.2483	0
Carp	−116.6180	0.172401	0	−0.169603	0	27.3840	0
Bleak	−95.9264	0.003779	1.63928×10^{-7}	−0.005028	1.66214×10^{-5}	2263.5700	23.4116
Roach	−113.332	0.000828	$1.19468 \text{x} 10^{-5}$	−0.002863	$8.64451 \text{x} 10^{-6}$	4981.3800	43.7143
Perch	−104.8510	0.006380	1.20771×10^{-4}	−0.026485	1.08995×10^{-4}	458.0280	4.1479
Trout	−78.3903	0.007256	3.6326×10^{-4}	−0.088649	5.54446×10^{-4}	132.9390	1.5685
Fish with two-chambered swimbladder	−109.2770	0.188982	0	−0.191582	0	24.1900	0
Fish with one-chambered swimbladder	−86.9923	0.010546	3.41879×10^{-4}	−0.080702	4.51678×10^{-4}	143.0690	1.4805
All fish	−108.8300	0.142688	4.76817×10^{-4}	−0.248634	7.30835×10^{-4}	24.1980	0

the surface of the swimbladder. Lobe accentuation increases with sound frequency (Love, 1977), and lobe number may be affected by the ratio of swimbladder length to acoustic wavelength L/λ (Johannesson and Mitson, 1983). In our experience, the lobes appeared to be symmetrical for any single fish (the lobes produced during the 0–180° rotation are mirrored by those produced during the 180–360° rotation) but no general pattern of lobes was found for other fish of the same size or species. It seems that the number, size, and location of lobes are unique for each individual fish, which is contrary to the expectations of Johannesson and Mitson (1983). The difficulty in determining the number of lobes was in defining the parameters that would clearly distinguish which peak or valley is a lobe and which is not. We tried different ways to find a pattern for identifying lobes and for relating lobe number to fish characteristics. For example, we attempted to identify lobes as all deviations larger or smaller then 3 dB from the regression model developed in this study (Tables 1 and 3) or as all TS fluctuations on the TS curve larger than 3 dB or 5 dB. Regardless of how lobes were defined, however, we found no relationship between lobe number and fish size.

In contrast to fish with two-chambered swimbladders, those with one-chambered swimbladders had no accentuation of lobes, which is consistent with the expectations of Horne et al. (2000). Relative to the TS pattern of two-chambered fish, however, the TS pattern of one-chambered fish had a stronger and narrower maximum peak in maximum aspect, TS minimum aspects near head or tail are less pronounced. Overall, the TS patterns of two-chambered fish were more regular than those of one-chambered fish (Figs. 1 and 2).

The observed U-pattern for TS for fish with one-chambered swimbladders and V-pattern for fish with two-chambered swimbladders correspond well with the independently chosen quadratic and linear models in Table 2. In addition, the R^2 values were greater for the quadratic model than for a previously studied sine model (Kubecka, 1994), although the quadratic model has the disadvantage of a more complex equation. One can, of course, find a slightly better fit with higher order polynomials for one certain fish but selection of a higher order polynomial will not generate equations with general application, i.e., with application for many species of fish. Furthermore, higher polynomials are less robust than simpler equations and may lead to the modeling of random artifacts in the data for one fish.

The difference in TS pattern between fish with one- and two-chambered swimbladders indicates that rather than describing a particular TS pattern for each fish species, researchers should identify general models that describe the TS pattern for the common one- and two-chambered European freshwater fish in any horizontal aspect. These general models would be useful for estimating fish size from horizontal acoustical records. When split-beam or multi-beam 3D sonars are used with accurate tracking in post-processing software (Balk and Lindem, 2000) to provide TS and fish aspect, the regressions in Table 3 could be used to estimate fish size.

Acknowledgements

This study was supported by grants no. 206/07/1392 of the Czech science foundation.

Authors thank Dr. Lars G. Rudstam for careful editing of the English text and inspirative questions.

References

Akaike, H., 1974. A new look at the statistical model identification. IEEE Trans. Automatic Control 19 (6), 716–723.

Balk, H., Lindem, T., 2000. Improved fish detection in data from split-beam sonar. Aquat. Living Resour. 13, 297–303.

Balk, H., Lindem, T., 2006. Sonar 4, Sonar 5, Sonar 6 – Post-processing Systems. Operator Manual. University of Oslo, Norway, pp. 427.

Francois, R.E., Garrison, G.R., 1982. Sound-absorption based on ocean measurements. Part I: Pure water and magnesium-sulfate contributions. J. Acoust. Soc. Am. 72 (3), 896–907.

Frouzova, J., Kubecka, J., Balk, H., Frouz, J., 2005. Target strength of some European fish species and its dependence on fish body parameters. Fish. Res. 75, 86–96.

Horne, J.K., Walline, P.D., Jech, J.M., 2000. Comparing acoustic model predictions to in situ backscatter measurements of fish with dual chambered swimbladders. J. Fish. Biol. 57, 1105–1121.

Horne, J.K., Clay, C.S., 1998. Sonar systems and aquatic organisms: matching equipment and model parameters. Can. J. Fish. Aquat. Sci. 55 (5), 1296–1306.

Jaffe, J.S., 2006. Using multi-angle scattered sound to size fish swimbladders. ICES J. Mar. Sci. 63 (8), 1397–1404.

Johannesson, K.A., Mitson, R.B., 1983. Fisheries Acoustics – A Practical Manual for Aquatic Biomass Estimation. FAO Fisheries Technical Paper-T240, 249, ISBN: 9251014493.

Knudsen, F.R., Seagrov, H., 2002. Benefits from horizontal beaming during acoustic survey: application to three Norwegians lakes. Fish. Res. 56, 205–211.

Kubecka, J., 1994. Simple model on the relationship between fish acoustical target strength and aspect for high-frequency sonar in shallow water. J. Appl. Ichthyol. 10, 75–81, 1397–1403.

Kubecka, J., Wittingerova, M., 1998. Horizontal beaming as a crucial component of acoustic fish stock assessment in freshwater reservoirs. Fish. Res. 35, 99–106.

Lilja, J., Marjomaki, T.J., Riikonen, R., Jurvelius, J., 2000. Side-aspect target strength of Atlantic salmon (*Salmo salar*), brown trout (*Salmo trutta*), whitefish (*Coregonus lavaretus*) and pike (*Esox lucius*). Aquat. Living Resour. 13, 355–360.

Love, R.H., 1977. Target strength of an individual fish at any aspect. J. Acoust. Soc. Am. 62 (6).

McClatchie, S., Alsop, J., Ye, Z., Coombs, R.F., 1996. Consequence of swimbladder model choice and fish orientation to target strength of three New Zealand fish species. ICES J. Mar. Sci. 53 (5), 847–862.

Pedersen, G., Handegard, N.O., Ona, E., 2009. Lateral aspect, target strength measurements of in situ herring (*Clupea Harengus*). ICES J. Mar. Sci. 66 (6), 1191–1196.

Pena, H., Foote, K., 2008. Modelling the target strength of *Trachurus symmetricus* murphyi based on high-resolution swimbladder morphometry using an MRI scanner. ICES J. Mar. 65 (9), 1751–1761.

Simmonds, D.M., MacLennan, E.J., 2005. Fisheries Acoustics: Theory and Practice. Blackwell, Oxford, UK.

Tuser, M., Kubecka, J., Frouzova, J., Jarolim, O., 2009. Fish orientation along the longitudinal profile of the Rimov reservoir during daytime: consequences for horizontal acoustic surveys. Fish. Res. 96 (1), 23–29.

Yasuma, H., Takao, Y., Sawada, K., Miyashita, K., Aoki, I., 2006. Target strength of the lanternfish, *Stenobrachius laucopsarus* (family Myctopidae), a fish without an airbladder, measured in the Bering Sea. ICES J. Mar. Sci. 63 (4), 683–692.

Yasuma, H., Sawada, K., Ohshima, T., Miyashita, K., Aoki, I., 2003. Target strength of mesopelagic lanternfishes (family *Myctopidae*) based on swimbladder morphology. ICES J. Mar. Sci. 60, 584–591.